Intercomparison of Spectroradiometers for Global and Direct Solar Irradiance in the Visible Range

JOSÉ A. MARTÍNEZ-LOZANO, MARIA P. UTRILLAS, ROBERTO PEDRÓS, AND FERNANDO TENA

Grupo de Radiación Solar, Universitat de Valencia, Valencia, Spain

JUAN P. DÍAZ AND FRANCISCO J. EXPÓSITO

Departamento Física, Universidad de La Laguna, Tenerife, Spain

JERÓNIMO LORENTE AND XAVIER DE CABO

Departamento de Meteorología y Astronomía, Universitat de Barcelona, Barcelona, Spain

VICTORIA CACHORRO AND RICARDO VERGAZ

Grupo de Óptica Atmosférica, Universidad de Valladolid, Valladolid, Spain

VIRGILIO CARREÑO

Estación Atmosférica de Izaña, Instituto Nacional de Meteorología, Tenerife, Spain

(Manuscript received 15 February 2002, in final form 20 November 2002)

ABSTRACT

This paper presents the results of the analysis of the spectral, global, and direct solar irradiance measurements in the visible range (400–700 nm) that were made in the framework of the first Iberian UV–visible (VIS) instruments intercomparison. The instruments used in this spectral range were four spectroradiometers: three Licor 1800s equipped with different receiver optics and one Optronic 754. For the direct solar irradiance measurements the spectroradiometers were equipped with collimators with different fields of view. Parallel studies have been carried out with the data given by the spectroradiometers with their original calibration file and with the same data that is corrected, following in situ calibration of the instruments using a laboratory reference lamp. To compare the series of spectral data the relative values of mean absolute deviation (MAD) and root-mean-square deviation (rmsd) have been used. The results obtained from the measurements of global irradiance show that the Licor 1800s presented very significant differences at the beginning and at the end of the day due to the deviation from ideal cosine response of the collection optics (i.e., cosine errors). This forced the analysis to be limited to the measurements corresponding to solar elevations higher than 30°. For this solar elevation range, the results of the intercomparison between the Licor instruments, before their in situ calibration, showed differences of about 5% in the visible range. The results from the measurements of direct irradiance show that, if correction factors are considered, these deviations are reduced to 3%, and when the Licors are compared with the Optronic, the deviations are less than 2%.

1. Introduction

In the framework of the research project CL197-0345-C05 (included in the Spanish National Program on Climate), supported by the Spanish Interministerial Commission of Science and Technology (CICYT), the first Iberian UV–visible (VIS) instruments intercomparison was carried out in September 1999 at the installations of the National Institute of Aerospace Technology (INTA) of El Arenosillo in Huelva, Spain. The main objective of this intercomparison was to know the state of most of the instruments that were used to measure the spectral UV solar radiation in Spain and Portugal, but because some of these instruments also measure in the visible spectrum, the intercomparison was extended to the visible range in such cases.

This paper summarizes the results of the analysis made in the visible range from global and direct spectral solar irradiance measurements in the intercomparison. All of the results refer to the 400–700-nm spectral range. Although the instruments that were used permit the ac-

Corresponding author address: José A. Martínez-Lozano, Grupo de Radiación Solar, Departamento de Termodinámica, Universitat de València, Dr. Moliner 50, Burjassot 46100 Valencia, Spain.
E-mail: jmartine@uv.es

quisition of data in part of the near-infrared (IR) range, it was decided to not include this in the analysis for two reasons because (a) the IR interval of the instruments is small, reaching, in the best case, up to 1100 nm, so that the results could not be considered as very representative of the IR range; and (b) the limit of the IR range of the different instruments is not the same, so if we wanted to draw conclusions that are valid for all of the instruments we would have had to limit the spectral interval at 800 nm.

To our knowledge there have been no previous intercomparison exercises such as this, based on solar irradiance in the visible range, because the instruments that are usually used for spectral irradiance measurements in this range are normally calibrated via Langley's regression or against a laboratory reference lamp (Kiedron et al. 1999). Although a similar intercomparison exercise was carried out for Licor 1800 spectroradiometers at the Solar Energy Research Institute (SERI) in 1987 (Riordan et al. 1990), the results are not available (Myers 1994, personal communication). In this work we have followed, in the visible range (as far as possible), the procedures used in the UV-range intercomparison campaigns that were carried out in recent years (Gardiner and Kirsch 1995; Webb 1997; Seckmeyer et al. 1998; Bais et al. 2001).

2. Description of the intercomparison campaign

One of the activities established in the working program of the coordinated research program CLI97-0345-C05 was a spectral radiometer intercomparison in the UV and visible ranges. Initially the instruments included in the intercomparison were those of the groups participating in this research program, that is, the National Institute of Meteorology (INM), INTA, and the Universities of Barcelona, Valencia, and Valladolid. Due to the interest of other research groups, the intercomparison was opened to other institutions of Spain and Portugal.

Simultaneous UV and VIS outdoor measurements were performed under different atmospheric conditions. The measurements were blind in order to assess objectively the performance of the instruments; none of the participants exchanged data during the measurement stage. An independent referee supervised the intercomparison and collected the measurement data directly from the operators of each instrument. This role was assumed by J. Gröbner, from International Ozone Services, Inc., Toronto, Ontario, Canada. In addition to the outdoor solar irradiance measurements, a series of lamp measurements were carried out in the laboratory for calibration and characterization of the spectroradiometers. Another objective was to familiarize some of the participants with the intercomparison procedures and the interchange of problem analysis and ideas about instrumentation and measurement methods.

The intercomparison took place from 31 August to 10 September 1999 in the Centro de Experimentación de El Arenosillo (CEDEA) of the INTA. The CEDEA is located 33 km from the city of Huelva, Spain. Technical coordination was prepared by INM, and local facilities and soundings were provided by CEDEA. The geographic coordinates of the CEDEA are 37°10′N, 6°73′W, and its height is 41 m above sea level. There are various factors that are critical to success in selecting an intercomparison site: climate, absence of obstructions (local and skyline) to the field of view (FOV), operational effectiveness, control room facilities, etc. (Bais et al. 2001). The CEDEA site satisfied these requirements perfectly. The location is beside the sea, close to the Strait of Gibraltar, and within the Doñana Natural Park in Huelva (one of the most important wetlands in the Iberian Peninsula, and possibly Europe). It is centered in an area that is completely flat, with Mediterranean pine and a horizon devoid of obstacles. During the outdoor intercomparison, all of the instruments were installed on the roof of the building with the same unobstructed field of view. The characteristics of the measurement site, as well as the overall meteorological conditions during the measurement campaign, are described in Sanchez et al. (2002).

The participating instruments were the following: eight Brewer (two MK-IIs, three MK-IIIs, and three MK-IVs), one Dobson, one Optronic 754, two Bentham 150, one Oriel MS257, and three Licor 1800 spectroradiometers. In this paper only the results corresponding to the measurements in the visible range obtained from the Licors and the Optronic are presented.

3. Instrumentation

For the purposes of the intercomparison in the visible range three Licor 1800s and one Optronic 754 spectroradiometers were used. The Licor 1800s have the following serial numbers: RS-312 (from Barcelona University), RS-415 (from Valencia University), and RS-487 (from Valladolid University). In the following text these instruments are referred to as the Barcelona University Licor (BAL), Valencia University Licor (UVL), and Valladolid University Licor (VAL). The Optronic 754 has the serial number 98202085. It is operated by the Valencia University and in the following work is referred to as the University of Valencia Optronic (UVO).

The Licor 1800 is a spectroradiometer equipped with a single monochromator that allows measurements in the 300–1100-nm range, with a FWHM of approximately 6 nm and a 1-nm wavelength step. The receiver in UVL and BAL is a Teflon diffuser and that of the VAL is a remote cosine sensor with a fiber optic probe. The Optronic 754 is equipped with a double monochromator, with a spectral range that extends from 250 to 800 nm and a FWHM of 1.6 nm, allowing measurements to be made with a minimum wavelength step of 0.05 nm. The detector is a solid-state photomultiplier

TABLE 1. Main instrument details.

	Licor 1800	Optronic
Entrance optic	Ptfe (Telflon) cosine diffuser	Integrated sphere OL-IS-670
Quality measured	Irradiance	Irradiance
Instrument	RS-312/RS-415/ RS-487	754-98202085
Focal length (mm)	—	160
Grating, groove (mm^{-1})	800	1200
Slit dimensions (nm)	0.5	0.25
Filter trip point (nm)	299, 348, 418, 558, 678, 775, 938	290, 345, 602
Wavelength range (nm)	300–1100	280–800
Resolution (FWHM) (nm)	6.25	2
Sampling step (nm)	1	0.05
Detector	Silicon photodiode	Photomultiplier Optronic S-20
Calibration standard	1800-02L/ORL815	OL 752-10E/OL 752-150
FOV for direct measurements (°)	4.7 (UVL)/ 4.2(VAL)	5.7
Alignment for direct measurements	Manual	Manual

with a temperature stabilized by the Peltier effect. The UVO receiver is equipped with an integrating sphere for the measurement of global irradiance. The main specifications of all the instruments used are listed in Table 1, which was based on similar criteria to those that appear in other recent publications in this field (i.e., McKenzie et al. 2002).

Several papers have studied the uncertainty of the Licor 1800 spectroradiometer (Riordan et al. 1989; Nann and Riordan 1991; Lorente et al. 1994; Cachorro et al. 1998). The errors with this type of instrument are due as much to the calibration process (lamp and alignment) as to the measurements (wavelength shift, cosine response, temperature, slit function, stray light, nonlinearity of the detector, and random). The overall uncertainty is obtained from the root-square sum. The measurement error with these instruments depends on the spectral region considered. The greatest errors (around 20%) correspond to the ultraviolet B (UVB) range, due primarily to the very broad slit function and single monochromator (i.e., stray light). In the visible and near-infrared regions (400–1000 nm) the error in the irradiance, governed by the calibration and measurement uncertainties, is 5% (see Table 2), while in the range between 1000 and 1100 nm, the error can increase significantly because of the sensitivity of the spectroradiometer to external temperature. The errors for UVO are determined mainly by the calibration process (see Table 2).

The sources of uncertainties can be divided into two groups: calibration and measurement. In the first group we include the errors due to the traceability of the lamps from national standard laboratories [the National Institute of Standards and Technology (NIST) in this work], and the errors associated with the calibration procedures

TABLE 2. Value of the errors involved in the measurement of the irradiance with the different spectroradiometers for the visible range.

Source of uncertainty	Uncertainty (%) UVO	UVL	VAL
Calibration lamp	±2.5	±2.5	±2.5
Alignment measurements	±0.5	±0.5	±0.5
Shift of the wavelength scale	±1.0	±1.0	±1.0
Cosine response systematic	±2.0	±2.5	±2.5
Temperature	±1.0	±2.5	±2.5
Slit function	±0.5	±1.0	±1.0
Stray light	±0.2	±1.5	±1.5
Nonlinearity of the dector	±0.2	±0.5	±0.5
Random	±1.0	±1.5	±1.5
Overall uncertainty (root-square sum)	±3.7	±5.0	±5.0

that were performed in home laboratories. We have no control over the first kind of error. The problem in the calibration procedure is to achieve a perfect alignment between the lamp and instrument's input optics port and to maintain a constant predefined current across the lamp filament. The error associated with the traceability of the lamps is given by NIST. The uncertainty in the management of the lamp depends strongly on the design of the home laboratory and the experience of the operator. This error has been obtained by considering the error in the stability of the current across the lamp and the error in the position calculated by the inverse distance square law. The laboratory setup is described in section 5. A complete description of error sources in the measurement procedure can be seen in Zerefos and Bais (1997), Gardiner and Kirsch (1995), and Koskela (1994). The measurement errors in Table 2, except for the temperature, have been obtained from the manufacturer and the above-mentioned literature. The error in the temperature was calculated using a temperature-controlled chamber to illuminate the instrument with a current-controlled standard calibration lamp.

For the direct irradiance measurements, collimators were used that had different FOVs. The collimators of the Licor 1800s were designed and constructed by each of the groups that operate them, based on a design previously developed at the SERI (Cannon 1986). The UVO collimator was supplied with the instrument by the manufacturers. In the UVL and BAL cases, in order to carry out the direct measurements, a collimator is attached directly over the instruments' entrance. The measurements are made by mounting the complete spectroradiometer on a tripod with a three-axis ball-and-socket joint that allows the collimator to be pointed and incorporates a sun-pointing viewfinder. In the VAL case the collimator is directly adjusted over the remote cosine sensor, which is mounted on the tripod and ball-and-socket joint. In the UVO the integrating sphere's mobility is used (it can rotate through 360° over the optical head's input). In this case the collimator is coupled to the entrance of the integrating sphere, having previously removed its quartz dome. As for the UVL and the VAL,

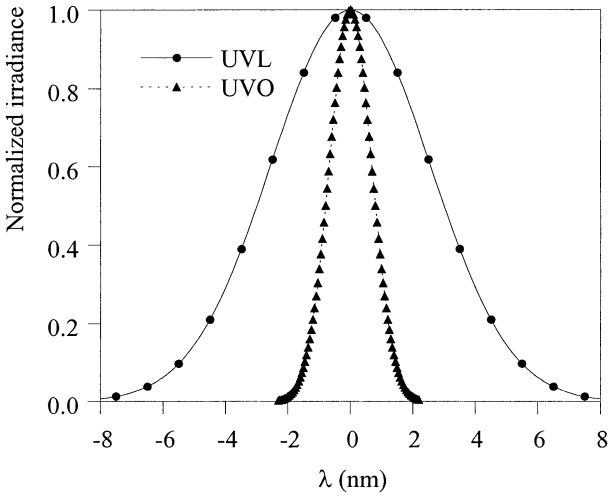

FIG. 1. UVL and UVO slit functions.

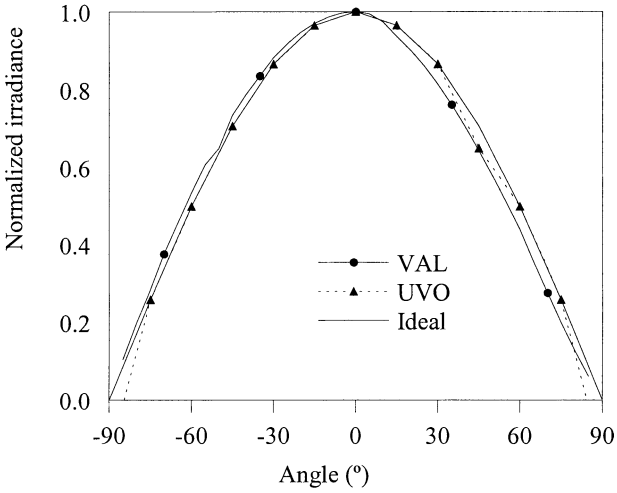

FIG. 2. Cosine response of the UVO and VAL with the remote cosine detector in the entrance.

it is the entire spectoradiometer that is mounted on the tripod and ball-and-socket joint.

In order to be able to apply the wavelength-shift algorithms to the intercomparison data, they must be referenced to the same aperture function. For this, the usual procedure is to evaluate the aperture function (as commented on below), deconvoluting the measurements, and then to convolute with the same aperture function for all of the instruments. The aperture functions of all the instruments are determined in the laboratory by shining fixed-wavelength radiation on the spectroradiometer and measuring a series of very close wavelengths. Because we did not have a source of monochromatic UV, as an alternative the emission peaks of an Hg fluorescent lamp were used. In the case of the UVO, the measurements were made without applying the calibration file to the maximum resolution of the instrument (0.05 nm) around the peak of 253.65 nm. The increase in the background signal with wavelength is due to emission by the reflective covering of the lamp and leads to a nonsymmetric aperture function. In Fig. 1 the UVO aperture function is shown with the 0.2 mm $\times$ 1.0 mm $\times$ 0.25 mm grid and aperture configuration. The Gaussian adjustment function, obtained by applying Bais's (1977) recommendations, gave a correlation coefficient of 0.9973 and a FWHM of 1.9 nm. In the case of the Licors, the entry and exit grids, both of which are 0.5 nm, gave an FWHM value of 6 nm. Figure 1 shows the aperture function of the UVL using a Gaussian adjustment distribution. In our opinion, the Licors compensate their limited precision (e.g., with respect to that of the UVO) with their ease of installation, transportability, and handling, as well as their stability, robustness, and their function/price relation. They are routinely used by the participating groups in the intercomparison, basically for determining the atmospheric components (especially aerosols) from extinction measurements of solar direct irradiance (Cachorro et al. 1998, 2000; Gröbner et al. 2001; Lorente et al. 1994; Martínez-Lozano et al. 1998, 2001, 2002).

When the instruments are compared from the global irradiance measurements, the cosine response can be one of the principal causes of discrepancies in the measurements, which is why it is important to adequately characterize it. The behavioral deviations, given by the expression

$$E_\lambda(\text{meas}) = E_\lambda(\text{real})\cos\theta, \tag{1}$$

are called cosine error, and normally tend to underestimate the measured signal, particularly for low sun elevation values. This cosine error is usually characterized with the expression

$$R_c(\lambda) = \frac{\displaystyle\int_{(2\pi)} L(\lambda, \theta, \varphi)C(\lambda, \theta, \varphi)\sin\theta\, d\theta\, d\varphi}{\displaystyle\int_{(2\pi)} L(\lambda, \theta, \varphi)\cos\theta\sin\theta\, d\theta\, d\varphi}, \tag{2}$$

where φ is the azimuth angle of the incident radiation, $L(\lambda, \theta, \varphi)$ is the incident spectral radiance, and $C(\lambda, \theta, \varphi)$ is the angular response of the input optics, normalized to 1 for $\theta = 0$. Ideally, the angular response would have to equal to $\cos\theta$. In Fig. 2 are shown the cosine responses of the UVO (with integrating sphere) and VAL (with the remote cosine sensor), as determined in the laboratory.

Finally, the possible wavelength shift in the spectroradiometric measurements has been considered. Normally the wavelength alignment of a spectroradiometer is calibrated either by measuring the emission lines of a lamp whose line positions are known to a precision of ± 0.001 nm (Gröbner et al. 1998), or by analyzing the entire measured spectrum according to the position of the Fraunhofer lines in the measured spectrum (Huber et al. 1993). This calibration is based on a limited num-

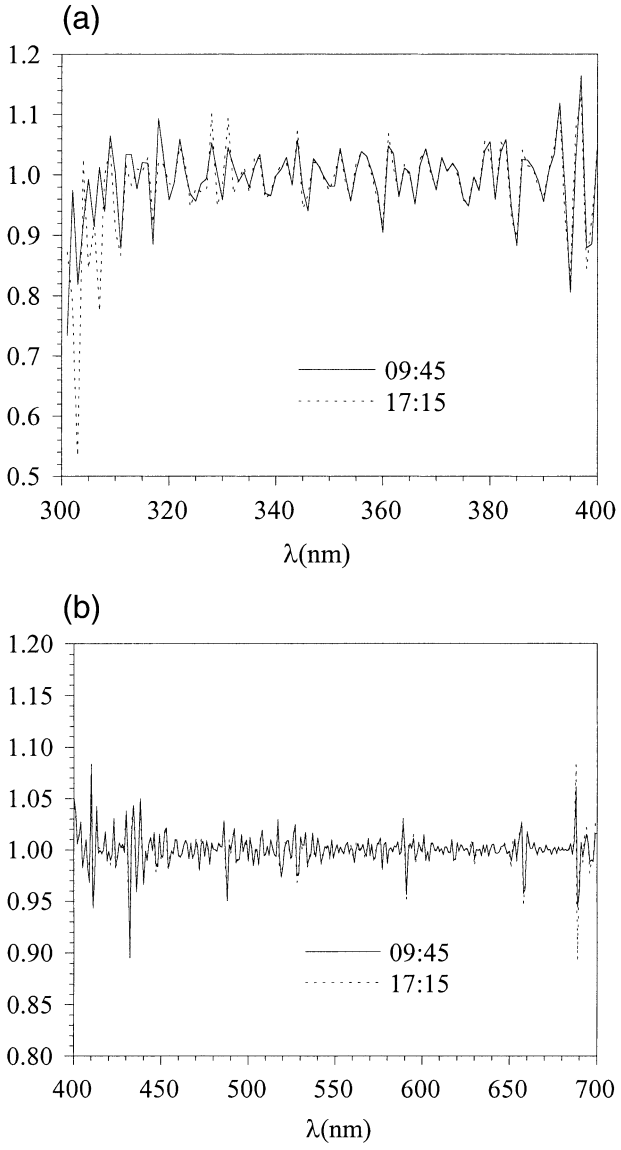

FIG. 3. Ratio values for two spectral measurements at different times in the same day from UVO in the (a) UV and (b) visible range.

ber of lines, so its application at intermediate wavelengths could introduce errors, should the monochromator show nonlineal behavior. This is not the case because, according to the manufacturer, the UVO linearity is of the order of ± 0.2 nm.

However, the measurements made during the intercomparison campaign showed that, in the UV range, there was a wavelength shift of nearly 1 nm through the day due to temperature variations. This effect, which has been previously reported by other authors (Slaper 1997; Seckmeyer et al. 1998), is due to the dilations that occur in the holographic diffraction gratings that are not temperature stabilized, unlike the detector, which is stabilized for the Peltier effect. In the UV range the algorithm of Slaper et al. (1995) can be used with a reference spectrum for extraterrestrial solar irradiance obtained from the solar ultraviolet spectral irradiance monitor (SUSIM) instrument (van Hoosier et al. 1988). The extraterrestrial solar irradiance spectrum is a stable reference that can be used for analyzing, a posteriori, any wavelength shift. Given that in the UV measurement range a 0.5-nm wavelength step is used, it is absolutely essential to correct for this wavelength shift to avoid introducing serious errors in the comparison.

In order to determine whether a correction of this sort was needed in the visible range, the method for wavelength shift determination proposed by Slaper et al. (1995), based on the $R_M(\lambda)$ factor, was used, analyzing the evolution along the day of this factor in the visible range. The $R_M(\lambda)$ factor is defined by the expression (Slaper et al. 1995)

$$R_M(\lambda) = 2M(\lambda)/[M(\lambda - s) + M(\lambda + s)], \qquad (3)$$

where $R_M(\lambda)$ is the ratio of the measurement at wavelength λ, with two close neighbors; $M(\lambda)$ is the measurement at wavelength λ; and s is the wavelength step between the central and two surrounding measurements. The $R_M(\lambda)$ ratio allows the stability of measurements of close wavelengths with respect to the shift due to the thermal dilation of the monochromator to be tested. The determination of the wavelength shift by using lamps, following the procedure proposed by Gröbner et al. (1998), would have been advisable. However, this must be carried out at different controlled temperatures in the laboratory in order to establish a function that describes the wavelength shift due to thermal dilation. Unfortunately, no such controlled temperature system was available, for the range of temperatures obtained during the day, throughout the intercomparison campaign.

Figures 3a and 3b show an example of the values of this parameter for two measurement series, taken with a time difference of more than 7 h, in the UV (Fig. 3a) and the visible (Fig. 3b) parts of the spectrum. From graphs like these it is possible to analyze the shift due to temperature variations during the day. As can be seen, the $R_M(\lambda)$ factor has considerably higher values in the UV than in the visible range. The comparison of these values with the ratio of the extraterrestrial measurement at wavelength λ, with two close neighboring wavelengths, showed that in the visible range the wavelength shift never reached 1 nm. Given that the measurements of the Optronic spectroradiometer were made in this spectral interval with a 1-nm wavelength step, and that the resolution of the Licor is very much less than this value, it was considered unnecessary to introduce this correction when comparing the Optronic measurements with those of the Licor 1800. The influence of the wavelength shift is particularly negligible for the latter instruments given the width of the aperture function (6 nm).

4. Uncertainty related with the use of the collimators in the direct solar irradiance measurements

It is important to point out that the measurements of direct irradiance are affected, in relation to the global irradiance measurements, by an additional factor leading to inaccuracies—the FOV of the different collimators used. The FOV of the VAL is 4.2°, that of the UVL is 4.7°, while that of the Optronic is 5.7°. Furthermore, for direct measurements all spectroradiometers were positioned manually, though this pointing accuracy was not quantified. The uncertainty related with the use of the collimators can be quantified by finding the order of magnitude of the error owing to the circumsolar radiance incident on the spectroradiometer detector. We have considered this uncertainty in three independent ways. This section discusses these three approaches using the Valencia University Licor for illustration.

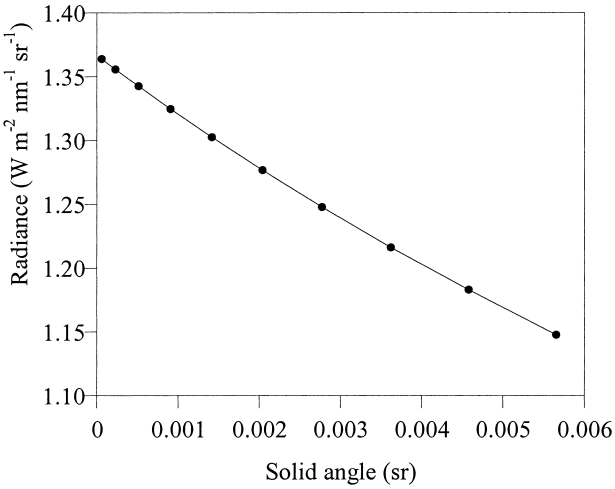

FIG. 4. Derived radiance values at 500 nm using the SKYRAD.PACK algorithm at 1000 UTC 7 Sep 1999.

a. Radiative transfer equation (RTE) method

We have used the Nakajima SKYRAD.PACK code (Nakajima et al. 1983, 1996). This code is the most widely used in recent years [e.g., the aerosol robotic network (AERONET); Holben et al. 1998]. The main source of error in this model comes from the imprecise a priori characterization of the atmospheric aerosols. In our case, we get around this problem by introducing the real aerosol optical thickness (AOT), determined previously (e.g., see methodology in Martínez-Lozano et al. 2001), to solve the RTE. Applying this algorithm, we have determined the radiance for the zenith angle ranging from 0.2° to 2.4°. The lower limit corresponds to half of the angle that the sun spans, and the upper limit corresponds to half of the collimator FOV of the UVL. The radiance values, estimated using the SKYRAD.PACK code at every chosen azimuth angle, and the corresponding solid angle, at 1000 UTC 7 September 1999, are shown in Fig. 4. Assuming that the sky radiance is a continuous function of the solid angle, we integrated the data to obtain the circumsolar irradiance fraction (at 500 nm) incident on the detector.

We wanted to obtain the contribution of the sky radiance to the measured irradiance, due to the fact that the solid angle subtended by the collimator is higher than the solid angle subtended by the sun. Because the sky radiance varies with the azimuth angle, using the SKYRAD.PACK code, we obtained the values for the range of azimuth angles from 0.2° to 2.4° every 0.2°. The limits were chosen to exclude the sun and to cover the entire collimator FOV. Once the radiances had been calculated, we needed to obtain their corresponding solid angles, subtended on the detector. Multiplying the sky radiance (in every zenith angle) with the subtended solid angle yields the sky irradiance. The radiance over the sky dome is a continuous function of the zenith angle (and thus of the solid angle on the detector). Therefore, we can obtain the total sky irradiance by integrating the radiance function (whose values are the SKYRAD.PACK outputs) over the solid angle. This value, for 500 nm, was 0.007 W m^{-2} nm^{-1}.

This quantity has to be subtracted from the irradiance measurements made using the spectroradiometer and the collimator. The solar direct irradiance on 7 September 1999 at 500 nm was 1.238 W m^{-2} nm^{-1}. Therefore, the inaccuracy due to the circumsolar radiation was 0.6%. The circumsolar radiation at 500 nm of 0.007 W m^{-2} nm^{-1} assumes that the sun is perfectly centered in the instrument FOV. When the sun is not in the center, then circumsolar radiation would probably be slightly less, as well as the inaccuracy due to this radiation.

b. Parametric method

Another approximation for this problem is given by the Gueymard (1995, 2001) parametric algorithm. This code allows the user to apply a parametric model in order to correct the circumsolar irradiance, taking into account the optical geometry of the system (slope, opening, and aperture angles). The circumsolar irradiance detected by the radiometer results from the spatial integration of the spectral sky radiance within the total field of view of the radiometer. Because the circumsolar radiance varies strongly with the scattering angle, but only slightly with azimuth, the azimuthally averaged radiance that exits along the almucantar is conventionally used to avoid a double angle integration over the aureole. The circumsolar irradiance detected by the radiometer is then

$$E_{dc\lambda} = 2\pi \int_0^{\xi_l} L_{a\lambda}(\xi) P(\xi) \sin\xi \cos\xi \, d\xi, \qquad (4)$$

where $L_{a\lambda}(\xi)$ is the azimuthal radiance that exits along

the almucantar, ξ is the incidence angle, and ξ_1 is the limit angle.

Applying the Gueymard model at 1000 UTC 7 September 1999 gave the circumsolar radiation due to the Licor collimator as 0.002 W m^{-2} nm^{-1}. This implied a less than 0.2% inaccuracy in the irradiance, which has the same order of magnitude as that obtained in the previous section.

c. Experimental method

A third approach appears in Myers (1994, personal communication). The precision of outdoor measurements and the total uncertainty of the calibration were calculated for different optical configurations of the Licor 1800 (Teflon dome, integrating sphere, and collimator). The results showed that the total measurement uncertainty at 500 nm was less than 4% using the collimator. In the same exercise, the total measurement uncertainty at 500 nm without a collimator was 3%. Therefore, the additional inaccuracy was about 1%, the same order of magnitude as in the two previous sections.

In order to summarize these results, we have to choose between the two different options that quantify the inaccuracy by either (a) assigning a new value for the spectroradiometer and collimator inaccuracy that would account for the collimator inaccuracy, whatever the aerosol content or type; or (b) maintaining the estimate for the accuracy and adding the value obtained from the SKYRAD.PACK calculations, which depends on the circumsolar radiation, which in turn depends on the aerosol content and type. In our opinion the latter option is more rigorous, and the authors have determined AOT inaccuracy accordingly in previous papers (e.g., Martínez-Lozano et al. 2002).

5. In situ spectroradiometer calibrations using spectral standard lamps

The main methods employed to establish an absolute irradiance scale are absolute cryogenic radiometry, synchrotron radiometry, and blackbody cavity radiometry. These techniques are used in national standards laboratories, such as NIST the National Physical Laboratory (NPL; United Kingdom) and Physikalisch-Technische Bundesanstalt (PTB; Germany). In an operative way the absolute scale irradiance must be transferred to the field instruments via intermedial sources and detectors. At present, the most widely used method to transfer the calibration is the spectral irradiance lamps. It is very important to take into account that relative accuracies of 1%–5% are attainable by well-maintained instruments, but absolute accuracies of better than 5% cannot presently be demonstrated due to the uncertainties introduced during the transfer of the absolute scale.

To calibrate a spectroradiometer using a spectral standard lamp is necessary to reproduce the same conditions in which the lamp was calibrated. Thus, it is extremely important to maintain the accuracy and precision of the distance between the optical input of the instrument with regard to the lamp filament, its vertical alignment, and the lamp current throughout the calibration process. The setup used in the laboratory measurements achieves the requirements with regard to the distance and alignment between the lamp filament and the optical input of the instrument. It consists of a vertical bench with three holders: one for the calibration lamp, a second one on the top of the bench for a laser, and a third one on the bottom holds a baffle. The calibration instrument is placed over a base with its sensor in the vertical position of the lamp and laser. A 3D-axis holder is used for the lamp, which can be adjusted by 3-μm screws. The laser at the top of the bench is a 10-mW He–Ne laser, which permits the vertical alignment between the lamp and the optical input of the instrument. To ensure this alignment, a small mirror is placed (in the equipment with a plane diffuser as input) over the diffuser. The lamp and the input of the equipment will be in the same vertical, whether the glint of the laser light reaches the output window of the laser source. One of the more important parameters in this setup is the distance between the input of the instrument and the lamp filament. Note that following the distance square inverse law, a difference of 1 mm in 500 mm, which is the usual distance between the lamp and the sensor, gives an error of 0.5% in the absolute irradiance. To fix this distance a nondeformable 50-cm bar has been used. All of the fine adjustments were done with micrometer screws in the three space directions.

The current across the lamp is another of the main factors that is necessary to reproduce exactly in order to calibrate any instrument. This intensity must be accurately maintained during all of the calibration period at the same value. Note that for a 1000-W FEL lamp, an error of 0.1% in the current produces an error of 1% in the spectral irradiance at the wavelength of 300 nm. In order to always reproduce the same intensity a current-control system has been developed. A 1800-W Sorensen 150-12B supplies the power to the circuit. This source works between 0 and 150 V, and it can be externally controlled by a control voltage (0–10 V) with a factor conversion of 1/15. This power supply can follow a voltage $\pm 0.03\%$ with variations in the charge. It has a response to the transients of 50 ms, although this response decreases for frequencies lower than 60 Hz in a factor of $(60/f)^2$. Moreover, it has a typical resolution of $\pm 0.05\%$. The Sorensen source has two work modes: voltage and current. In the first mode the voltage is constant, whereas the current varies with the charge. In the second one the voltage varies and the current is constant. The source can change automatically between both modes, depending on the charge. In this current-control system the source has been controlled by an external voltage input, which it has permitted to change the set-point voltage in the voltage mode. In order to control this power supply a dedicated PC with an an-

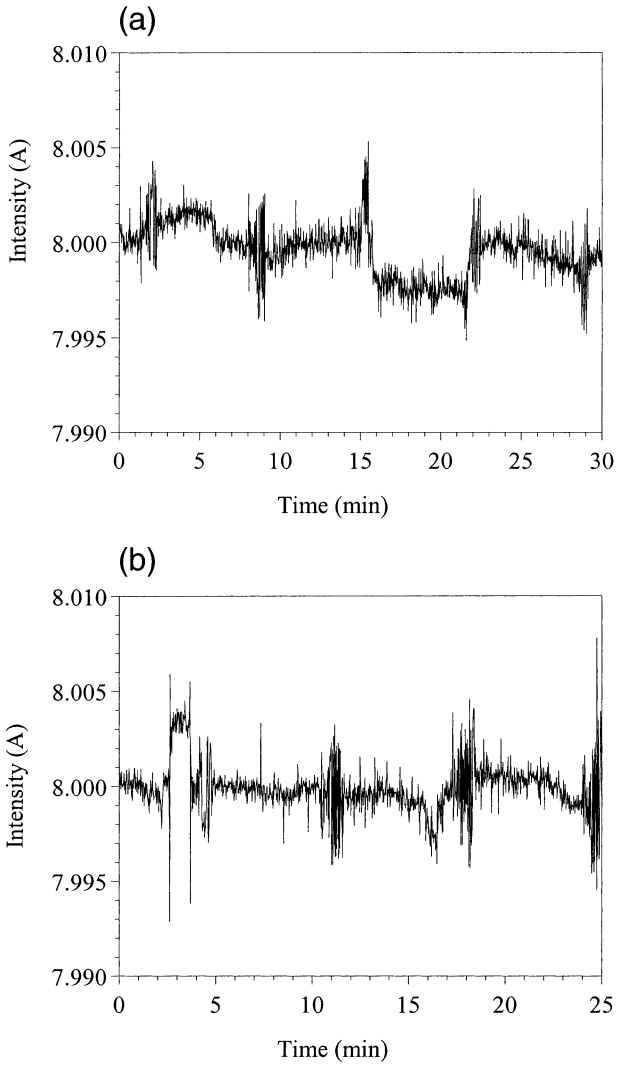

FIG. 5. Intensity across the filament of the standard lamp: (a) UVO and (b) UVL.

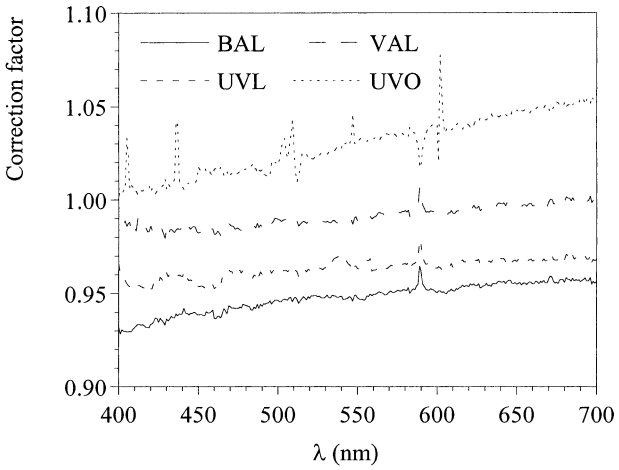

FIG. 6. Correction factors for the spectroradiometers in the visible range obtained from the calibration against the reference lamp.

alog–digital/digital–analog (ADDA) card has been installed. This card permits the appropriate voltage signal to be sent to the Sorensen to control the current of the lamp. This signal depends on the voltage measured by a precision voltmeter in the terminal of a high-precision resistor (shunt). The voltmeter is six digits and half HP 34401A, with output HP-IB and RS-232. Following Ohm's law, this instrument measures the current in the circuit via the shunt and continuously sends these data to the PC using the serial port. In order to check the aging of the lamp it is important to record these data and the voltages in its ends. Moreover, the analysis of these records will permit the validation of the calibration, because any abnormal variation in the irradiance must be followed by a variation in the current. In the software used during this intercomparison the control is based in the last three voltages measured across the shunt. The command sent to the power supply tries to correct the difference between the setting current and the value measured using a weighted function of the last three differences. The weights are 60% for the last value, 25% for the value before the last, and 15% for the first one. This strategy, although it does not correct the white noise of the natural oscillations of the circuit, reduces the scattering of these data.

The absolute calibration of the instruments was carried out during 3 days (6–8 September) using two NIST traceable lamps (lamps 85 and 95) and a seasoned one (4). Figures 5a and 5b show the data of intensity recorded for the UVO and UVL instruments, respectively. During the calibration, the calibration factors were obtained for the different spectroradiometers against the reference lamps.

On the days before the intercomparison campaign all of the spectroradiometers that measure in the visible range were calibrated in the laboratories of their respective groups. The Licors were calibrated using the calibration system developed by Licor (Licor Optical Radiation Calibrator), whose source is a 200-W halogen–tungsten lamp, calibrated at a color temperature of 3150 K with respect to the NIST working standard. The manufacturer guarantees a response change of less than 1% during 50 h of use. The power supply of the lamp provides a precision of $\pm 0.1\%$. For the calibration of the UVO for global irradiance measurements, the system provided by Optronic is used. This consists of a support for the calibration lamp and a stabilized power supply. The support allows the integrating sphere to be coupled to the instrument with controlled alignment and distance. The power supply has a resolution of 0.01 V and 0.001 A, giving a voltage precision for the lamp of $\pm 0.001\%$, at the current used. The manufacturer provides the working standard spectral irradiance, a 200-W tungsten lamp operating at 6.5 A. From their new spectral responses, determined in situ, the spectroradiometers' correction factors have been calculated for application to the experimental data. These factors, which are presented in Fig. 6, were obtained from the cali-

bration factors of the different spectroradiometers against the reference lamps and the calibration files obtained in the laboratory of each of the participating groups.

In Fig. 6 it is seen that for the UVO the average deviation was 0.4%. The smallest Licor's deviations from the original calibration correspond to the VAL, with a median value of approximately 1.0%, while the values corresponding to the BAL and UVL instruments were 5.4% and 3.5%, respectively. The authors note that because the instruments are calibrated by measuring the radiation of a calibration lamp placed at the calibration distance from the radiometers' entrance optics, the exact measurement of this distance is critical in the calibration process. In the VAL case, because of the configuration of the optics, this measurement is easily made. However, this is not the case for the BAL and UVL because the Teflon diffuser is curved, so it is not obvious to which point inside the entrance optics the distance should be measured. This could cause significant uncertainty (depending on the calibrated distance) in the spectroradiometer's calibration factor (Bernhard and Seckmeyer 1997). The principal sources of uncertainty in the calibration processes are 1) the uncertainty associated with the NIST traceability (NIST uncertainty) and 2) the uncertainty due to the transfer (transfer uncertainty). The latter covers the error in the power supply as well as that due to the lamp's position. Since the intercomparison was performed, Hofzumahaus et al. (1999) have presented a method that allows the effective planar receptor (EPR) of a curved entrance optic to be determined by calibrating at several distances and using the inverse square law to solve for the EPR. This correction is fundamental for equipment with dome-type entrance optics, such as those described by Hofzumahaus et al. (1999). However, for equipment that includes diffusers, like the Licors, their influence is much less, because these diffusers can be considered almost flat.

6. Results for global irradiance

During 3 and 4 September 1999 global solar irradiance on a horizontal plane was measured every 15 min from 0630 to 1745 UTC. On the first day all four instruments were used. On the second day the Optronic 754 was used just to measure UV irradiance with a higher-precision wavelength step, so measurements are only available for the three Licor 1800 instruments for this day. So that the results obtained for all the instruments would be comparable, a 1-nm band step was used (the smallest permissible for the Licors). In all of the cases two scans were performed, and the average of the two was stored. The time used in all of the measurement processes was not more than 50 s. The results from all the Licors have been intercompared and each of these has been compared in turn with the Optronic 754. The first analysis carried out was for the data registered by the spectroradiometers, using their respective calibration files obtained in their groups' laboratories (original or uncorrected data).

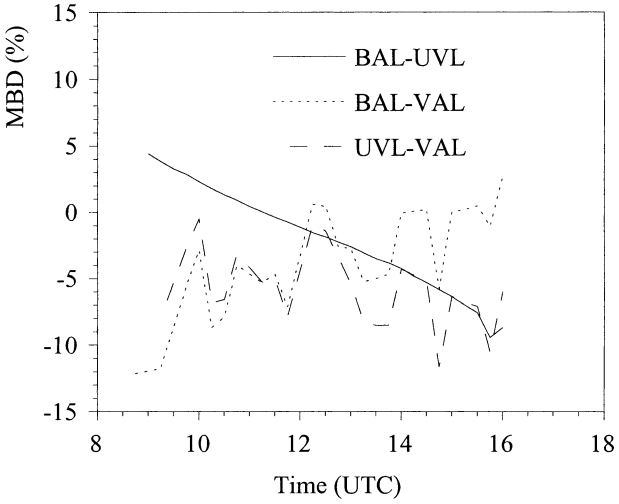

FIG. 7. Daily evolution of the relative MBD (%) on 3 Sep 1999. Comparison of Licor–Licor with original experimental data. Solar elevation >30°.

Once the new calibration factors have been established, these have been used to correct the experimental data that was analyzed previously (processed or corrected data). To compare the series of spectral data, the relative values (%) of mean absolute deviation (MAD), mean bias deviation (MBD), and root-mean-square deviation (rmsd) have been used. To condense the results only the averages of the differences for each spectral measurement series are presented. These average values were obtained from the 300 values corresponding to each wavelength step between 400 and 700 nm.

a. Intercomparison between the Licor 1800s

The 2 days (3 and 4 September 1999) for which measurements of the global horizontal irradiance were made have been analyzed separately. Figure 7 shows, as an example, the daily evolution of the average values of the relative (%) MBD for the uncorrected (original) data of 3 September 1999. These values were obtained from the set of the spectral values in the 400–700-nm range. In this figure it can be seen how at the beginning of the morning and at the end of the afternoon the values of MBD are much higher than in the middle of the day. This is due basically to the error introduced by the cosine effect in the global irradiance measurements on a horizontal plane for low solar elevation angles.

In order to obtain representative statistical indicators of the relative MBD, MAD, and rmsd parameters for each of the days, we have ignored the extreme hours, focusing on the interval between 0800 and 1600 UTC, to avoid the distortions introduced by the cosine effect. On these days 0800 UTC corresponded to a solar elevation of 23° and 1600 UTC to a solar elevation of 30°

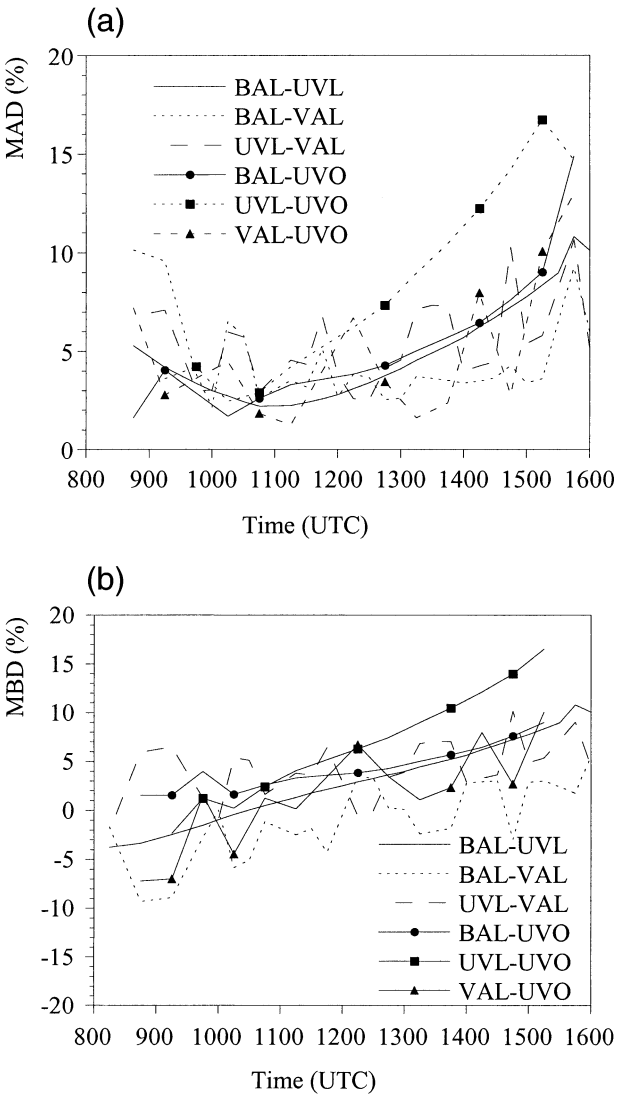

FIG. 8. Daily evolution of the relative (a) MAD (%) and (b) MBD (%) on 3 Sep 1999. Corrected experimental data. Solar elevation >30°.

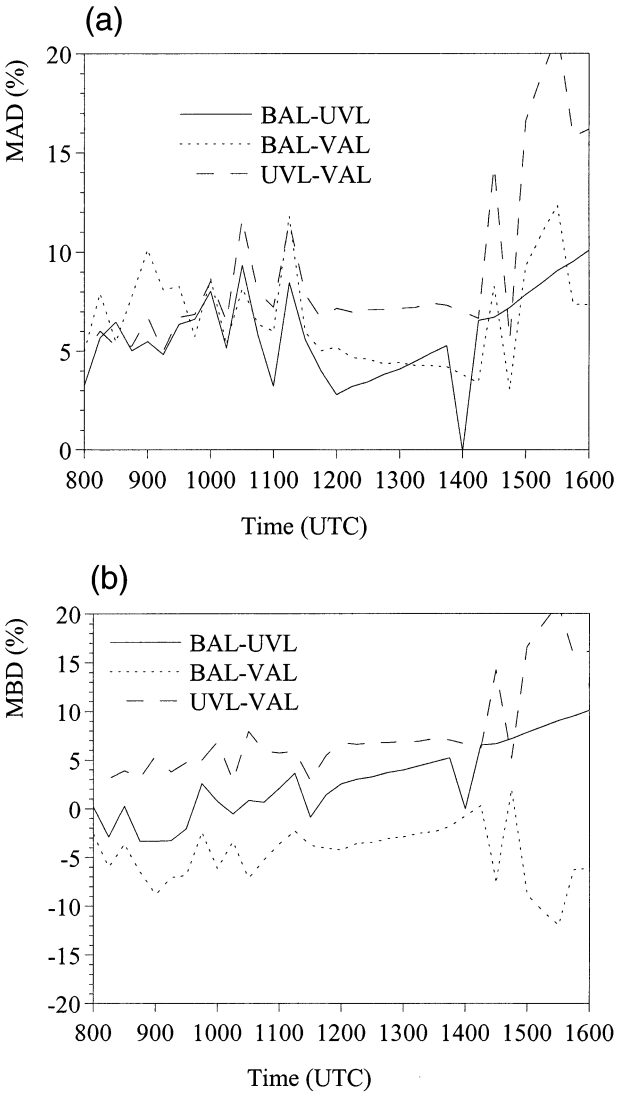

FIG. 9. Daily evolution of the relative (a) MAD (%) and (b) MBD (%) on 4 Sep 1999. Corrected experimental data. Solar elevation >30°.

(equivalent to an optical mass of approximately 2). In order to maintain symmetry with respect to solar noon, we have used only values corresponding to solar heights of over 30° (optical mass 2) in the calculations, so that all of the conclusions will only be valid for optical masses less than this value. This assumes that the average values of the daily spectral MAD were obtained from 32 spectra, each of which corresponded to 300 wavelength values. Figures 8 and 9 present the daily evolution of the average values of relative (%) MAD and MBD for 3 and 4 September 1999 after correcting the experimental values (corrected data). The curves given in these figures show that the variations in the differences throughout the day are smoother for UVL and BAL and less stable for VAL, especially on 3 September 1999. In summary, Table 3 presents the median values

TABLE 3. Medium values of relative MAD (%) and relative rmsd (%) for Licor–Licor comparison for UC and C values.

	MAD (UC)	Rmsd (UC)	MAD (C)	Rmsd (C)
	Day 3 Sep 1999			
BAL − UVL	3.8	4.0	3.9	4.0
BAL − VAL	5.8	5.9	2.7	2.8
UVL − VAL	7.2	7.3	4.4	4.6
	Day 4 Sep 1999			
BAL − UVL	5.4	5.8	5.7	6.4
BAL − VAL	10.2	10.5	5.9	6.7
UVL − VAL	10.0	10.5	7.6	8.0

for MAD and rmsd for the uncorrected (UC) and corrected (C) experimental data for each of the measurement days (corresponding to solar elevations above 30°). From Table 3 we can see that if we consider MAD as an indicator of nonsystematical deviations, then in no case do the corrected values pass 8%, even on 4 September 1999. These results, although difficult to generalize, seem to indicate the appropriateness of the Licors for this type of measurement so long as the solar zenith angle (SZA) is less than 60°.

b. Comparison of the Licor 1800s with the Optronic 754

We present here the results obtained by comparing the measurements made with the Optronic 754 with those from each of the Licors. The procedure has been totally analogous to the one described in the previous section, but limited only to 3 September 1999. In this case we present only the results obtained from the corrected data using the calibration factors obtained in the laboratory against those obtained by the reference lamp. In Figs. 8a and 8b, the daily evolution of the relative average values of MAD and MBD obtained from the corrected experimental data can be seen for 3 September 1999.

The curves that appear in these figures show some significant differences with respect to those in figures corresponding to the intercomparisons of the Licors. First, the differences in the early and late hours are smoother, but also, the symmetry that was found in the previous case disappears. Instead, there is a tendency for the difference to increase through the day in the cases of UVL and BAL. In fact, we see the UVL and BAL behaving differently from that of VAL. The curves corresponding to UVL and BAL are smoother, as was the case when the Licors were compared among themselves, which could be explained by the influence of the fiber optic probe (its movement and change of input optics) on the stability of the measurements through the day. On the other hand, the values of MAD and MBD of the VAL stay within a narrower margin over the length of the day than the values for the other two, which tend to increase. This asymmetry around midday cannot be interpreted solely in terms of the cosine effect and must necessarily be due to other causes. All of this appears to indicate that in these spectroradiometers, and particularly in UVL, in addition to the cosine effect, there is another effect that has not been taken into account so far. In our opinion this effect, temporal and asymmetric, has to be a consequence of the temperature effect on the Licors and the Optronic; although, in this case it ought to affect the VAL also. One possible explanation of why this effect is much less noticeable in the VAL could be the following. On 3 and 4 September 1999 the UVL and BAL operated automatically, exposed to the sun throughout the day on their tripod mountings. The VAL was operated manually with a fiber optic probe. The VAL remote cosine sensor was located on a tripod while the Licor itself remained at ground level. The operational procedure consisted of the acquisition of the direct and global measurements alternately. This meant there was a presence of at least one and, for much of the time, two operators from the University of Valladolid standing close to the Licor to handle the remote cosine sensor. In this way, although the VAL was not expressly protected from the sun's rays, it is very likely that during some of the time it was in shadow. The different influence of temperature on the VAL is not reflected in the Licor–Licor intercomparison, so perhaps the explanation of this phenomenon is not so simple. Nevertheless, and in the absence of a more convincing reason, it would seem that the use of the fiber optic probe had two opposite effects: on the one hand, it introduced variations in the MAD of up to 7% between consecutive measurements, but on the other hand, given the method of operation of the instrument during the campaign, it could have favored the protection of the detector from the temperature effect.

TABLE 4. Median values of relative MBD (%), MAD (%), and relative rmsd (%) for Optronic–Licors comparison on 3 Sep 1999.

	MBD	MAD	Rmsd
Uncorrected values			
UVO − BAL	5.5	6.1	6.5
UVO − UVL	3.6	6.6	6.7
UVO − VAL	−1.1	4.2	4.9
Corrected value			
UVO − BAL	3.3	3.8	4.1
UVO − UVL	4.1	7.1	7.0
UVO − VAL	1.2	4.0	5.1

Table 4 shows the values of the median of MBD, MAD, and rmsd parameters for each of the instruments compared with the Optronic. The values in this table were calculated, as in the previous cases, using only the experimental data corresponding to solar elevations greater than 30°. The table shows that, although all of the values could be considered as acceptable, those corresponding to VAL were significantly lower that those for UVL and BAL (about 30% lower). Furthermore, in the cases of these latter two instruments, the differences were not uniform through the day (a fact that is not reflected in the table). If only the experimental values corresponding to the morning are considered (until 1200 UTC), then the MAD (%) is reduced to 3.8 for the BAL and 4.5 for the UVL. This confirms that there is some time-dependent external parameter that is not related to the solar elevation that influences the differences between these two instruments and the UVO.

7. Results for direct irradiance

The measurements of direct irradiance were made on 7 September 1999, and the employed instruments were the VAL, UVL, and UVO. An important difference with

TABLE 5. Statistical values of relative MBD (%), MAD (%), and rmsd (%) for UVL–VAL comparison on 7 Sep 1999.

	MBD	MAD	Rmsd
	Uncorrected values		
Min	−8.8	1.6	1.6
Max	−1.6	8.8	8.9
Mean	−4.9	4.9	5.3
Median	−5.1	5.1	5.4
	Corrected values		
Min	−7.3	1.1	1.6
Max	0.3	6.0	6.3
Mean	−2.6	2.3	3.0
Median	−2.0	2.4	3.0

respect to the measurements of global irradiance is that in this case, to avoid the effect that temperature had on the Optronic, an attempt was made to protect the instruments as much as possible from direct exposure to the sun's rays; and during the whole measurement period the UVL and UVO were protected with reflecting plastic. This strategy was not followed during the measurements of global irradiance, because the wavelength shift due to the temperature detected in the UVO was diagnosed during the measurements made in the laboratory using the reference lamps. As previously indicated, the days on which these measurements were made were intermediate days between the days when the global measurements were made and the days when the direct measurements were made. Furthermore, and because their operation was manual in this case, they were kept in the shade between measurements. The results suggest that these protective strategies were sufficient to limit the main temperature effect.

The procedure followed to analyze the results was the same as described above for the horizontal global irradiance. The only difference is that in this case, all of the available measurements were used, without the limitation related to the solar elevation, because the cosine effect is irrelevant when measuring direct irradiance. We present first the comparison of the two Licors and then the results of the comparison of these instruments with the UVO. Only the results deduced from the processed data obtained after correcting for the calibration factors measured in the laboratory against the reference lamps are analyzed.

Table 5 presents the maximum and minimum values, as well as the average and the median of MBD, MAD, and rmsd parameters. They are less than those found for measurements of global irradiance, despite the differences in the FOVs. The average rmsd is of the order of 3% for the entire visible range. This allows us to affirm, with the caveat given at the start of this section, that the Licors are adequate instruments for measuring direct solar irradiance, and the results that they give are comparable, even when the optics of the receiver and the FOV of the collimator are different.

Figure 10 presents the ratios between the average

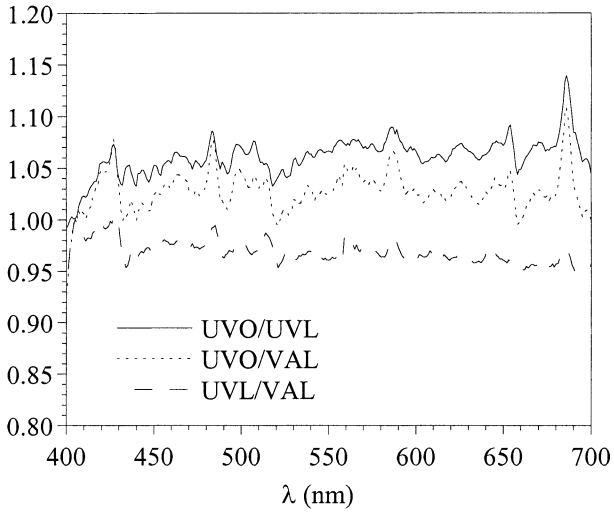

FIG. 10. Ratio of the direct irradiance measurements (daily mean) from each pair of instruments used in the intercomparison on 7 Sep 1999 for the visible range.

experimental measurement values, corresponding to the comparison in the visible range. Figure 11 shows the daily evolution of these ratios for the 500-nm wavelength. From these figures and the MBD results shown in Table 5, we can conclude that the UVL data are overestimated relative to the Optronic, while the VAL data are underestimated. The differences between the values given by the three instruments are practically constant except around 1400–1430 UTC, at which time there appeared a pronounced peak with no obvious explanation. This peak was also apparent when the two Licors were compared.

Table 6 gives the median values of MBD, MAD, and rmsd of the UVL and VAL in comparison with the UVO.

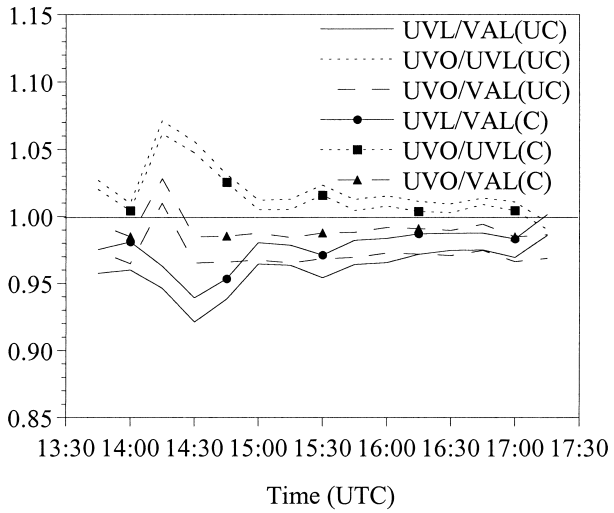

FIG. 11. Daily evolution of the ratio of the direct irradiance at wavelength 500 nm for each pair of instruments used in the intercomparison on 7 Sep 1999 for UC and C values.

TABLE 6. Median values of relative MBD (%), MAD (%), and rmsd (%) for UVO–Licors comparison on 7 Sep 1999.

	MBD	MAD	Rmsd
Uncorrected values			
UVO − UVL	1.3	1.6	2.2
UVO − VAL	−3.2	5.2	4.1
Uncorrected value			
UVO − UVL	1.0	1.9	3.1
UVO − VAL	−1.1	1.6	3.1

A very good agreement is seen in both cases, exceptionally so for the UVL. All of the differences are of the same order or less than the instruments' accuracies, so it is not possible to draw valid conclusions with respect to one or the other instrument. However, it is interesting to note that the drift in time of the value of the differences, observed in the measurements of global irradiance, is not seen in the direct irradiance. This allows us to reaffirm our hypothesis that they were due to the temperature effect and that they were not seen in this case because of the protective measures taken. Furthermore, the variations in time in form of a sawtooth that appeared in the global irradiance measurements from the VAL do not appear either, which seems to confirm that they could have been caused by horizontal alignment errors of the remote cosine sensor.

8. Conclusions

We have analyzed the results obtained from the measurements of global and direct solar irradiance in the visible range (400–700 nm), registered during the first Iberian UV–VIS instruments intercomparison, which took place from 31 August to 10 September 1999 in the Centro de Experimentación de El Arenosillo (CEDEA) of the National Institute of Aerospace Technology (INTA). The instruments used were three Licor 1800 spectroradiometers and one Optronic 754 spectroradiometer. During the measurements of direct irradiance an attempt was made to protect the instruments from direct exposure to the sun's rays. The results indicate that the measurements taken were sufficient to remove the temperature effect. To compare the series of spectral data, relative values of MAD and rmsd were used.

The results of the analysis of the measurements of global irradiance showed that the Licor measurements suffered significant distortions at the beginning and end of the day, due to the cosine effect. This forced us to limit the analysis to the measurements corresponding to solar elevations of higher than 30°. For this solar elevation range, the results of the intercomparison between the Licor spectroradiometers, before their in situ calibration, showed differences that were 5% in the visible range, and that were greater when one of the instruments (the Licor) had a fiber optic probe. We think that the greater discrepancy between this and the other two instruments could be due to a combination of the use of the fiber optic probe and the manual operation of the instrument. Once the calibration factors obtained against a reference lamp had been applied, the results related to the VAL improved noticeably, to around 3%, while those of the BAL and UVL remained practically unchanged. These results could be related to the procedure used during the laboratory calibration, because the Teflon diffuser has a curved geometry that could lead to significant uncertainty in the calibration factor.

The comparison between the Licors and the Optronic, using uncorrected data from in situ calibration, showed an asymmetry between the morning and afternoon results for the BAL and UVL, possibly due to the temperature effect. The results with the VAL were noticeably better, perhaps due to differences in the measurement procedure. Although the VAL continued to show the variations noted previously, the average difference was less. Once the calibration factors obtained from the reference lamp were applied, the results from the BAL improved significantly, while those of the UVL and VAL remained practically unchanged. This suggests that the UVL is subject to a temperature effect similar to the Optronic, but so far this effect has not been quantified.

The results of the analysis of the measurements of direct irradiance showed that, even when considering uncorrected data, the differences between the Licors were of the order of the accuracy of these instruments in the visible range. When correction factors are considered the differences reduced to 3%. The comparisons with the Optronic gave figures of 5% for the VAL and 2% for the UVL, for uncorrected data. After correcting the data, the average differences were less than 2% in both cases. These results could be considered as exceptional, given that the instruments are each mounted with collimators with different FOVs and each has different optics in the receiver. In our opinion these results justify the use of the Licors for the acquisition of highly reliable measurements of direct irradiance in the visible range.

Finally, we wish to indicate that the results obtained with the Licor when measuring global irradiance, especially relative to the UVL, appear to show a previously unreported temperature dependence of these instruments. This dependence was not quantified during the intercomparison to which this paper refers, and will be studied in the near future within the frame of a new spectroradiometer intercomparison.

Acknowledgments. This work was financed by the Spanish CICYT through the CLI97-0345-C05-04 project. We would like to thank the collaboration of the members of all the participating teams in the intercomparison campaign, particularly to A. Redondas of the INM at Izaña, who was responsible for the intercomparison in the UV range that initially determined the drift of the Optronic with temperature. We would also like to show our thanks to B. de la Morena for all the

facilities put at our disposal in the El Arenosillo installations and to L. Sánchez-Muniosguren for coordinating this project.

REFERENCES

Bais, A. F., 1997: Spectrometers: Operational errors and uncertainties. *Solar Ultraviolet Radiation: Modelling, Measurements, and Effects,* C. S. Zerefos and A. F. Bais, Eds., NATO ASI Series I, Vol. 52, Springer-Verlag, 165–173.

——, and Coauthors, 2001: SUSPEN intercomparison of ultraviolet spectroradiometers. *J. Geophys. Res.,* **106,** 12 509–12 525.

Bernhard, G., and G. Seckmeyer, 1997: New entrance optics for solar spectral UV measurements. *Photochem. Photobiol.,* **65,** 923–930.

Cachorro, V. E., M. P. Utrillas, V. Vergaz, P. Durán, A. de Frutos, and J. A. Martinez-Lozano, 1998: Determination of the atmospheric-water-vapor content in the 940-nm absorption band by use of moderate spectral-resolution measurements of direct solar irradiance. *Appl. Opt.,* **37,** 4678–4689.

——, P. Durán, R. Vergaz, and A. de Frutos, 2000: Columnar physical and radiative properties of atmospheric aerosols in north central Spain. *J. Geophys. Res.,* **105,** 7161–7175.

Cannon, T. W., 1986: Spectral solar irradiance instrumentation and measurement techniques. *Sol. Cells,* **18,** 233–244.

Gardiner, B. G., and P. J. Kirsch, 1995: Setting standards for European ultraviolet spectroradiometers. European Commission Air Pollution Research Rep. 53, 138 pp.

Gröbner, J., D. J. Wardle, C. T. McElroy, and J. B. Kerr, 1998: An investigation on the wavelength accuracy of Brewer spectrophotometers. *Appl. Opt.,* **37,** 8352–8360.

——, R. Vergaz, V. E. Cachorro, D. V. Enriques, K. Lamb, A. Redondas, J. M. Vilaplana, and D. Rembges, 2001: Intercomparison of aerosol optical depth measurements in the UVB using Brewer spectrophometers and a Li-Cor spectrophotometer. *Geophys. Res. Lett.,* **28,** 1691–1694.

Gueymard, C., 1995: SMARTS2, a simple model of the atmospheric radiative transfer of sunshine: Algorithms and performance assessment. Florida Solar Energy Center Tech. Rep. FSEC-PF-270-95, 78 pp.

——, 2001: Parameterized transmittance model for direct beam and circumsolar spectral irradiance. *Sol. Energy,* **71,** 325–346.

Hofzumahaus, A., A. Kraus, and M. Müller, 1999: Solar actinic flux spectroradiometry: A technique for measuring photolysis frequencies in the atmosphere. *Appl. Opt.,* **38,** 4443–4460.

Holben, B. N., and Coauthors, 1998: AERONET—A federated instrument network and data archive for aerosol characterization. *Remote Sens. Environ.,* **66,** 1–16.

Huber, M., M. Blumthaler, and W. Ambach, 1993: A method for determining the wavelength shift for measurements of solar UV radiation. *Proc. SPIE,* **2049,** 354–357.

Kiedron, P. W., J. J. Michalsky, J. L. Berndt, and L. C. Harrison, 1999: Comparison of spectral irradiance standards used to calibrate shortwave radiometers and spectroradiometers. *Appl. Opt.,* **38,** 2432–2439.

Koskela, T., Ed., 1994: The Nordic intercomparison of ultraviolet and total ozone instruments at Izaña from 24 October to 5 November 1993. Final report. Finnish Meteorological Institute Tech. Report, Helsinki, Finland, 123 pp.

Lorente, J., A. Redaño, and X. de Cabo, 1994: Influence of urban aerosol on spectral solar irradiance. *J. Appl. Meteor.,* **33,** 406–414.

Martínez-Lozano, J. A., M. P. Utrillas., F. Tena, and V. Cachorro, 1998: The parameterisation of the atmospheric aerosol optical depth using the Ångström power law. *Sol. Energy,* **63,** 303–311.

——, ——, ——, R. Pedrós, J. Cañada, J. V. Boscá, and J. Lorente, 2001: Aerosol optical characteristics from a summer campaign in an urban coastal mediterranean area. *IEEE Trans. Geosci. Remote Sens.,* **39,** 1573–1585.

——, and Coauthors, 2002: A multi-instrument approach for characterizing the atmospheric aerosol optical thickness: Case study in the STAARTE/DAISEX-99 campaign. *Geophys. Res. Lett.,* **29** (4), 1053, doi:10.1029/2001GL013585.

Mckenzie, R., P. Johnston, A. Hofzumahaus, A. Kraus, S. Madronich, C. Cantrell, J. Calvert, and R. Shetter, 2002: Relationship between photolysis frequencies derived from spectroscopic measurements of actinic fluxes and irradiances during the IPMMI campaign. *J. Geophys. Res.,* **107** (D5), 4042, doi:10.1029/2001JD000601.

Nakajima, T., M. Tanaka, and T. Yamakuchi, 1983: Retrieval of the optical properties of aerosols from aureole extinction data. *Appl. Opt.,* **22,** 2951–2959.

——, G. Tonna, R. Rao, P. Boi, Y. Kaufman, and B. Holben, 1996: Use of sky brightness measurements from remote sensing of particulate polydispersions. *Appl. Opt.,* **35,** 2675–2686.

Nann, S., and C. Riordan, 1991: Solar spectral irradiance under clear and cloudy skies: Measurements and a semiempirical model. *J. Appl. Meteor.,* **30,** 447–462.

Riordan, C., D. Myers, M. Rymes, M. Hulstrom, W. Marion, C. Jennings, and C. Whitaker, 1989: Spectral solar radiation data base at SERI. *Sol. Energy,* **42,** 67–79.

——, ——, and R. L. Hulstrom, 1990: Spectral solar radiation data base documentation. Tech. Rep. SERI/TR-215-3513A, Golden, CO, 52 pp.

Sanchez, L., E. Cuevas, and B. de la Morena, 2003: *Results of First Iberian UV–VIS Instruments Intercomparison.* Ministerio de Medio Ambiente, in press.

Seckmeyer, G., and Coauthors, 1998: *The 1997 Status of Solar UV Spectroradiometry in Germany: Results from the National Intercomparison of UV Spectradiometers.* Shaker-Verlag, 166 pp.

Slaper, H., 1997: Methods for intercomparing instruments. Advances in solar ultraviolet spectroradiometry, European Commission Air Pollution Research Rep. 63, 155–164.

——, A. J. Reinen, M. Blumthaler, M. Huber, and F. Kuik, 1995: Comparing ground level spectrally resolved solar UV measurements using various instruments: A technique resolving effects of wavelength shift and slit width. *Geophys. Res. Lett.,* **22,** 2721–2724.

van Hoosier, M. E., J. D. F. Bantee, G. E. Braeckner, and D. K. Prinz, 1988: Absolute solar spectral irradiance 120–400 nm results from the SUSIM experiment on board Spacelab-2. *Astrophys. Lett. Commun.,* **27,** 163–168.

Webb, A. R., 1997: Advances in solar ultraviolet spectroradiometry. European Commission Air Pollution Research Rep. 63, 84 pp.

Zerefos, C. S., and A. F. Bais, Eds., 1997: *Solar Ultraviolet Radiation: Modelling, Measurements and Effects.* NATO ASI Series I, Vol. 52, Springer-Verlag, 332 pp.